Chin. Geogra. Sci. 2020 Vol. 30 No. 4 pp. 557–571
https://doi.org/10.1007/s11769-020-1135-y

Springer Science Press
www.springerlink.com/content/1002-0063

Different Responses of Vegetation to Frozen Ground Degradation in the Source Region of the Yellow River from 1980 to 2018

WANG Rui, DONG Zhibao, ZHOU Zhengchao

(*School of Geography and Tourism*, *Shaanxi Normal University*, *Xi'an* 710119, *China*)

Abstract: Frozen ground degradation under a warming climate profoundly influences the growth of alpine vegetation in the source region of the Qinghai-Tibet Plateau. This study investigated spatiotemporal variations in the frozen ground distribution, the active layer thickness (ALT) of permafrost (PF) soil and the soil freeze depth (SFD) in seasonally frozen soil from 1980 to 2018 using the temperature at the top of permafrost (TTOP) model and Stefan equation. We compared the effects of these variations on vegetation growth among different frozen ground types and vegetation types in the source region of the Yellow River (SRYR). The results showed that approximately half of the PF area (20.37% of the SRYR) was projected to degrade into seasonally frozen ground (SFG) during the past four decades; furthermore, the areal average ALT increased by 3.47 cm/yr, and the areal average SFD decreased by 0.93 cm/yr from 1980 to 2018. Accordingly, the growing season Normalized Difference Vegetation Index (NDVI) presented an increasing trend of 0.002/10yr, and the increase rate and proportion of areas with NDVI increase were largest in the transition zone where PF degraded to SFG (the PF to SFG zone). A correlation analysis indicated that variations in ALT and SFD in the SRYR were significantly correlated with increases of NDVI in the growing season. However, a rapid decrease in SFD (< −1.4 cm/10yr) could have reduced the soil moisture and, thus, decreased the NDVI. The NDVI for most vegetation types exhibited a significant positive correlation with ALT and a negative correlation with SFD. However, the steppe NDVI exhibited a significant negative correlation with the SFD in the PF to SFG zone but a positive correlation in the SFG zone, which was mainly limited by water condition because of different change rates of the SFD.

Keywords: permafrost; seasonally frozen ground; vegetation dynamics; climate change; source region of the Yellow River

Citation: WANG Rui, DONG Zhibao, ZHOU Zhengchao, 2020. Different Responses of Vegetation to Frozen Ground Degradation in the Source Region of the Yellow River from 1980 to 2018. *Chinese Geographical Science*, 30(4): 557–571. https://doi.org/10.1007/s11769-020-1135-y

1 Introduction

Frozen ground, including permafrost (PF) and seasonally frozen ground (SFG), has been recognized as a sensitive indicator of climate warming (Wang et al., 2018a). The degradation of frozen ground from rising temperatures is significantly influencing regional terrestrial ecosystem (Oliva et al., 2018; Wang et al., 2019a; Yang et al., 2019). For PF or perennially frozen ground, the subsurface temperature is at or below 0℃ for two or more consecutive years, and the near surface forms an active layer through the transition of seasons (Woo, 2012). SFG, as opposed to PF, refers to the minimum annual ground surface temperature is less than 0℃ and the shallow subsurface freezes and thaws annually (Barry and Gan, 2011). PF and SFG areas are distributed in different regions (Frauenfeld and Zhang, 2011; Lawrence et al., 2012), and have different geological fea-

Received date: 2019-08-14; accepted date: 2019-12-04

Foundation item: Under the auspices of National Natural Science Foundation of China (No. 41807061, 41930641, 41977061), Postdoctoral Science Foundation of China (No. 2018M633454), Team Building Research Funds for the Central Universities of China (No. GK202001003)

Corresponding author: DONG Zhibao. E-mail: zbdong@snnu.edu.cn.

tures (Gu et al., 2015), hydrothermal features (Evans and Ge, 2017), mechanical properties (Yang et al., 2015) and physical processes (Guo and Wang, 2013). Under a warming climate, both PF and SFG have experienced widespread degradation during the last several decades (Yang et al., 2019), which were characterized as variations in areal extent and depths of freezing/thawing (Wang et al., 2018b). The extent of PF/SFG in a region plays a key role in the distribution of surface-subsurface interactions (Zorigt et al., 2016). Both PF soils and seasonally frozen soils contain a surface layer that thaws and freezes seasonally, which is another estimated value that indicates changes in frozen ground; additionally, almost all hydrological, ecological, and biological activities occur within this layer (Wu et al., 2015; Gao et al., 2018).

Different types of underlying frozen ground exhibit different degradation processes (Guo and Wang, 2013; Mu et al., 2018), so the effects of changes within ecosystems cannot be accurately predicted. Many previous studies confirmed that permafrost degradation may negatively contribute to vegetation growth, such as a reduction in vegetation cover (Wang et al., 2012; Cable et al., 2014; Miranda et al., 2020), a decrease in the number of plant species (Yang et al., 2013) and the reverse succession of vegetation (Jin et al., 2009). In contrast, other studies found that warming permafrost was beneficial for vegetation growth through easing the freezing pressure (Yi et al., 2011; Feng et al., 2019). Qin et al. (2017) indicated that a decrease in the SFD could increase topsoil moisture, and promote the leaf area index during the initial period of a growing season. However, previous studies have been limited to investigating differences in the ecological effects between PF and SFG.

Additionally, heterogeneities in high-altitude cold regions result in different vegetation types with various bioecological characteristics. Anderson et al., (2019) classified three vegetation types in Interior Alaska in association with the ALT. The responses of vegetation to climate change differ according to the vegetation type. For example, warming can increase the coverage of deciduous shrubs and graminoids in alpine tundra (Walker et al., 2006), but decrease the coverage of low stature forbs, bryophytes and lichens in alpine grasslands (Klanderud, 2008). However, whether the responses to frozen ground degradation differ among different vegetation types has not been examined.

The Yellow River originates on the Qinghai-Tibet Plateau (QTP), which is a cold and arid region with a fragile ecosystem (Wang et al., 2017b; Shen et al., 2018). Because of the high altitude and climate of the source region of the Yellow River (SRYR), frozen ground is widespread and can be characterized as a transition region between PF and SFG (Jin et al., 2009). The vegetation in the SRYR is diverse, and alpine grassland is the primary vegetation type (Wang et al., 2019c). The development and stability of frozen ground provide a material basis for the maintenance of alpine grassland ecosystems (Yao et al., 2013), and the status and variations in frozen ground determine succession within alpine ecosystems (Wang et al., 2016; Oliva et al., 2018). Under a warming climate, the rate of temperature increase on the plateau has been obviously greater than that in other regions of the world in recent decades (Qin and Stocker, 2014); this trend has dramatically accelerated the degradation of frozen ground (Yang et al., 2019; Wang et al., 2019b). Therefore, understanding how frozen ground degradation affects the ecological environment in the SRYR is increasingly important, especially across different types of frozen ground and vegetation groups.

This study attempts to differentiate the effects of frozen ground degradation on vegetation growth among the types of the frozen ground and vegetation groups in the SRYR over the past few decades. We adopt the temperature at the top of permafrost (TTOP) model and the Stefan equation to simulate the distribution of frozen ground and the depths of soil freezing/thawing in the SRYR from 1980 to 2018 and assess the correlation with vegetation dynamics (1982–2015) as indicated by the normalized difference vegetation index (NDVI). The specific objectives of this study are as follows: 1) to investigate spatiotemporal variations in the growing season NDVI in relation to changes in the frozen ground distribution and depths of seasonal freezing and thawing (SFD and ALT); 2) to analyze relationships between frozen ground factors and NDVI by frozen ground types and vegetation groups.

2 Materials and Methods

2.1 Study area

The SRYR (32°10′N−36°59′N, 95°54′E−103°24′E) is a catchment above the Longyangxia Reservoir in the

mainstream area of the Yellow River, with an area of approximately 145 300 km^2 (Fig. 1). The SRYR features high plains, rugged mountains and hills, wide valleys, intermontane basins and numerous lakes. The altitude ranges from 6248 m in the Animaqin Mountains to 2427 m in the village of Tangnaga and decreases from west to east and south to north. The SRYR is characterized as a transition zone from permafrost to seasonally frozen soils at midlatitudes and high altitudes on the QTP (Jin et al., 2009). The SRYR has a typical continental plateau climate that is affected by the Asian monsoon, with an annual average temperature (AT) from −3.0 to −4.1℃ and an average annual precipitation of 300−700 mm.

2.2 Data

Daily AT, daily ground surface temperature, monthly precipitation, and maximum annual SFD for 11 meteorological stations in the SRYR and 12 stations near the SRYR over the period 1980−2018 were collected from the National Meteorological Information Center (http://data.cma.cn). The Gridded AT data were interpolated from the meteorological stations and the 30 m spatial resolution of the digital elevation model (DEM) by using the topographic adjustment method of our previous research (Wang et al., 2020). The Global Inventory Modeling and Mapping Studies (GIMMS, 1982–2006) and Moderate Resolution Imaging Spector radiometer (MODIS, 2002–2015) normalized difference vegetation index (NDVI) data were employed to examine the changes in vegetation cover over time. Using a linear fit between the two datasets for an overlapping data period (2000–2006) (Du et al., 2014), the relationship between them was applied to joint and extend the temporal sequence of the NDVI data. In this study, the spatial distribution of vegetation was extracted from the vegetation map of the People's Republic of China at a scale of 1 ∶ 1 000 000 (Hou, 2001). First, the vegetation of this study area from the vegetation map of China was clipped. Then, we categorized similar vegetation types into one based on the classification of each vegetation map. For example, the 'needle-leaved deciduous forest', 'needle-leaved evergreen forest', 'broad-leaved deciduous forest' and 'broad-leaved evergreen forest' were merged into 'forest'. The main vegetation types of the SRYR included alpine vegetation, meadow, grassland, forest, shrub and barren land (Table 1 and Fig. 2).

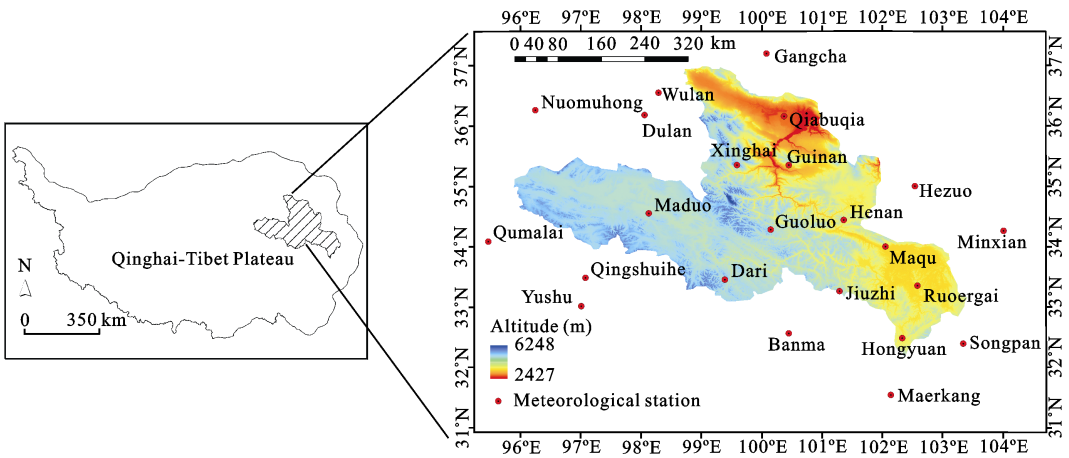

Fig. 1 General geographic map of the source region of the Yellow River and the distribution of the meteorological sites

Table 1 Description of vegetation types in the source region of the Yellow River

Vegetation type	Description
Forest	Needleleaf forests with dominant species *Picea crassifolia* and *Sabina przewalskii* in cold-temperate zones and mountains in temperate zones; broadleaf deciduous forests with dominant species *Populus davidiana* in temperate zones
Shrub	Subalpine broadleaf evergreen and deciduous shrubs with dominant species *Salix oritrepha* and *Caragana jubata*
Meadow	*Kobresia* spp., forb high-cold meadows with dominant species *Kobresia pygmaea*, *Stipa purpurea*, *Kobresia humilis* and *Kobresia schoenoides*
Steppe	Temperate tufted grass steppes with dominant species *Achnatherum splendens*, *Stipa breviflora* and *Stipa purpurea*
Alpine vegetation	Alpine sparse and cushion vegetation with dominant species *Saussurea* spp., *Rhodiola rosea*, *Cremanthodium* spp., and *Arenaria musciformis*
Barren land	Land without vegetation, such as permanent snow, glaciers and lake

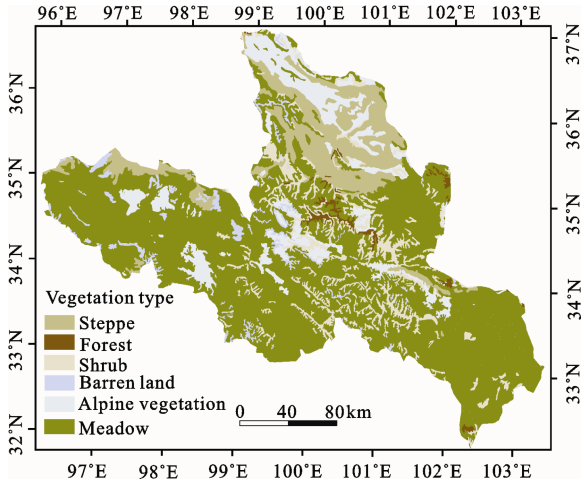

Fig. 2 Spatial distribution of vegetation types in the source region of the Yellow River

Surface soil moisture (SM) data for the SRYR over 2002–2011 were generated from the Advanced Microwave Scanning Radiometer-Earth Observing System (AMSR-E) instrument, which were provided by the National Snow and Ice Data Center (http://nsidc.org/). The Harmonized World Soil Database (HWSD) provieded the soil property data that includes the soil type, texture and bulk density (FAO and ISRIC, 2009). This study adopted the land cover map for the year 2000 with a 1-km spatial resolution (MICLCover 2000) that was produced through the International Geosphere-Biosphere Programme (IGBP) classification (Ran et al., 2012). The HWSD and MICLCover 2000 datasets were acquired from the Cold and Arid Regions Science Data Center at Lanzhou (http://westdc.westgis. ac.cn/).

2.3 Simulation of the frozen ground distribution

This study adopts TTOP model to simulate the spatial distribution of PF and SFG on the SRYR. This model is a semiphysical model and can be expressed as follows (Smith and Riseborough, 1996):

$$TTOP = \frac{\left(\frac{\lambda_t n_t TI_a}{\lambda_f}\right) - (n_f FI_a)}{t} \tag{1}$$

where $TTOP$ represents the mean temperature at the top of the PF or the temperature at the bottom of the active layer (℃); λ_t and λ_f represent the thermal conductivity of thawed soil and frozen soil (W/(m·K)), respectively; n_t and n_f represent the factors related to energy balance between the ground surface and near-surface atmospheres for the thawing period and freezing period, respectively; TI_a and FI_a represent the annual air-thawing index and annual air-freezing index (℃·d), respectively; and t represents the period that is 365 d for a regular year. According to the estimated $TTOP$ from 1980 to 2018, we discriminated the frozen ground distribution and subdivided the frozen ground into three types: PF ($TTOP \leq 0$℃), SFG ($TTOP > 0$℃) and the area where PF degraded into SFG (PF to SFG, $TTOP \leq 0$℃ in 1980s and $TTOP > 0$℃ in 2010s). The parameters in TTOP model and their processing details can be found in our previous studies (Wang et al., 2019a; 2019b; Wang et al., 2020). Additionally, the mean values of n_t and n_f were assigned to each land use type in SRYR. We calculated the n_t and n_f values at 23 meteorological stations for different land use types by using the observed ground surface temperature and AT from 1980 to 2018, which are listed in Table 2.

2.4 Estimation of the soil freezing/thawing depth

The depth of seasonal freezing and thawing, the ALT over the permafrost region and SFD of seasonally frozen soil were estimated by the Stefan equation (Wu et al., 2015), which is expressed as follows:

$$Z_A = \sqrt{\frac{2\lambda_t n_t TI_a}{\rho\omega_t L}}, \tag{2}$$

$$Z_S = \sqrt{\frac{2\lambda_f n_f TI_a}{\rho\omega_f L}}, \tag{3}$$

Table 2 The n_t and n_f values for each land-use type in the source region of the Yellow River

Land-use type	Areal ratio (%)	n_t	n_f
Grasslands	73.07	1.68	0.77
Farmlands	0.23	1.54	0.82
Barren or sparsely vegetated lands	16.35	1.72	0.64
Shrublands	3.28	1.62	0.78
Forests	0.53	1.64	0.80
Wetlands	1.84	1.42	0.85
Water bodies	3.88	—	—
Permanent snow and ice regions	0.82	—	—

Note: Water bodies and permanent snow and ice regions have no values of n_t and n_f because there are no meteorological stations

where Z_A and Z_S represent the ALT (m) and SFD (m), respectively; L represents the latent heat of fusion (3.34×10^5 J/kg); ω_t, and ω_f represent the average liquid soil water content during the thawing and freezing period (m^3/m^3), respectively; ρ represents the soil bulk density (kg/m^3); λ_t, λ_f, n_t, n_f, TI_a , FI_a, ω_t, ω_f and ρ were defined in Section 2.3 and introduced in our previous studies (Wang et al., 2019a; 2019b; Wang et al., 2020).

2.5 Statistical analysis

We used the trend line method to analyze the annual change rates of the ALT, SFD, growing season NDVI, and TTOP from 1982 to 2015 and the SM from 2003 to 2010 in each grid cell. Pearson correlation was used to analyze the spatial and temporal changes in vegetation growth responses to frozen soil variability. These analyses were conducted with the ArcGIS10.5 and MATLAB software.

3 Results

3.1 Validation with the observed data

The calculated extent of the frozen ground distribution, ALT and SFD were validated by point-scale observations. We collected data from boreholes that were drilled in 1988 and 2010 from previous studies in the SRYR for validation (Table 3). To evaluate the ALT, we compared the observations from the drilled boreholes and the results derived from the Stefan equation (Fig. 3a). The estimated ALT values had a significant linear relationship with the borehole observations (R^2 = 0.5802, root mean square error (RMSE) = 3.5047). Based on the observed frozen ground types of the boreholes, the types of most borehole sites were estimated accurately by the TTOP model (Table 3), except for two boreholes: K14 and K445.

Table 3 Borehole information from relevant previous studies in the source region of the Yellow River

Borehole	Lon. (N)	Lat. (E)	Alt (m)	Drilling time	Estimated type	Observed type	Reference
ZK5	34°53′	98°11′	4220	1988	PF	PF	Jin et al. (2009)
ZK6	35°05′	97°46′	4272	1988	PF	PF	
ZK7	35°12′	97°43′	4472	1988	PF	PF	
ZK8803	35°10′	97°42′	4400	1988	PF	PF	
ZK8804	35°01′	97°42′	4275	1988	PF	PF	
ZK8805	35°08′	97°45′	4300	1988	PF	PF	
No5	35°04′	98°05′	4239	1988	PF	PF	
No8	34°55′	98°31′	4253	1988	PF	PF	
No9	34°50′	98°08′	4216	1988	PF	PF	
No10	34°49′	98°22′	4218	1988	PF	PF	
K1	34°54′	96°20′	4583	1988	PF	PF	
K2	34°53′	96°20′	4507	1988	PF	PF	
K3	34°59′	97°48′	4272	1988	SFG	SFG	
K4	34°44′	96°09′	4557	1988	PF	PF	
K5	34°43′	96°09′	4569	1988	PF	PF	
K8	34°52′	98°10′	4211	1988	SFG	SFG	
K14	34°54′	98°11′	4221	1988	SFG	PF	
K10	34°01′	98°08′	4294	1988	PF	PF	
ZK4	34°00′	98°03′	4220	1988	SFG	SFG	
CLP-1	34°15′	97°51′	4727	2010	PF	PF	Luo et al. (2014)
CLP-2	34°15′	97°51′	4723	2010	PF	PF	
CLP-3	34°16′	97°52′	4663	2010	PF	PF	
CLP-4	34°19′	97°52′	4564	2010	PF	PF	
YNG-1	34°24′	97°57′	4452	2010	PF	PF	
YNG-2	34°26′	97°56′	4395	2010	SFG	SFG	
YNG-2	34°30′	97°58′	4333	2010	SFG	SFG	
XXH-1	34°39′	98°26′	4231	2010	SFG	SFG	
MDB	34°51′	98°33′	4225	2010	PF	PF	
K445	34°58′	98°33′	4288	2010	SFG	PF	

Notes: PF and SFG refer to permafrost and seasonally frozen ground, respectively

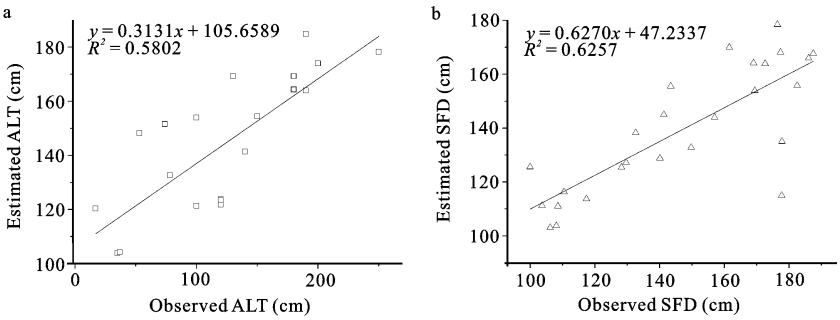

Fig. 3 Comparison of the estimated and observed active layer thickness of permafrost soil (ALT) (a) and the soil freezing depth of seasonal frozen soil (SFD) (b) in the source region of the Yellow River

The calculated SFD values were compared with observed values at 11 meteorological stations in the SRYR. Fig. 3b shows that the estimated SFD was significantly correlated with the observations (R^2 = 0.6257, *RMSE* = 2.8355). Therefore, the TTOP model and Stefan equation used in this study were applicable for simulating the frozen ground dynamics.

3.2 Comparisons of vegetation growth under different frozen ground types

Fig. 4 and Fig. 5 demonstrate the spatial distributions of decadal frozen ground area and the mean NDVI in the growing season from the 1980s to the 2010s. PF occurred in 40.40%, 37.56%, 24.71% and 20.03% of the SRYR in the 1980s, 1990s, 2000s and 2010s, respectively (Fig. 4). In a warming climate, the boundaries of the PF zone moved westward from 1980 to 2018. Approximately half of the PF degraded into SFG, with an average decrease rate of 5.22%/10a. The greatest change rate for the distribution of frozen ground extent occurred from the 1990s to the 2000s, whereas the lowest rate occurred from the 1980s to the 1990s. The region was classified into PF, SFG and PF to SFG by comparing the distributions of frozen ground between the 1980s and 2010s (Fig. 5). The areas of PF, SFG, and PF to SFG covered 2.91 × 10^4 km^2 (20.03%), 8.66 × 10^4 km^2 (59.60%) and 2.96 × 10^4 km^2 (20.37%) of the SRYR, respectively.

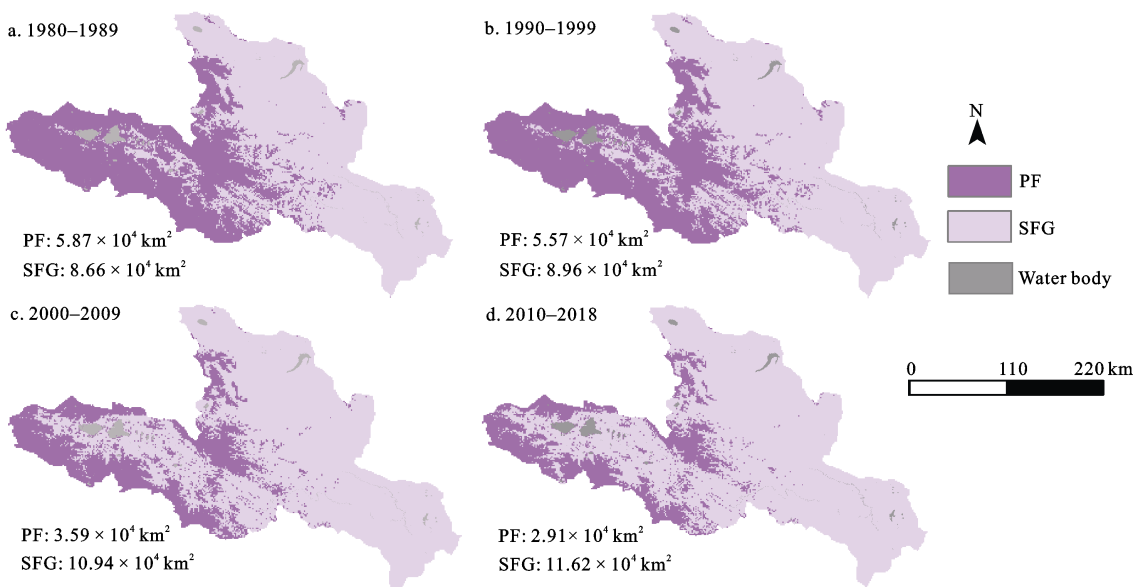

Fig. 4 Changes in the spatial distribution of frozen ground in the source region of the Yellow River in the periods of 1980–1989 (a), 1990–1999 (b), 2000–2009 (c) and 2010–2018 (d)

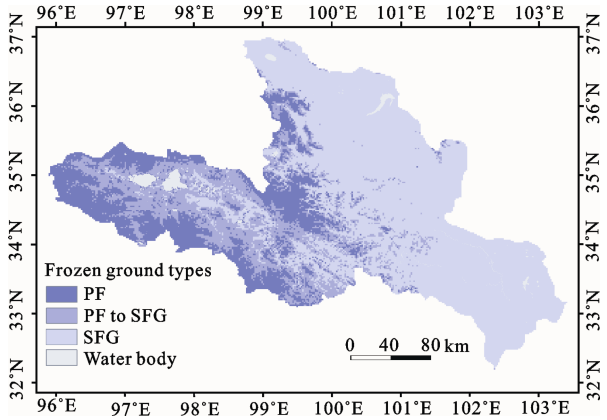

Fig. 5 Simulated frozen ground distribution in the source region of the Yellow River in 1980−2018

The mean annual values of the ALT in the PF zone and the SFD in the PF to SFG and SFG zones from 1980 to 2018 were 228.948 cm, 201.841 cm and 186.827 cm, respectively (Table 4). The SFG zone, which was located in the southeastern SRYR and had the lowest altitude, exhibited the largest mean NDVI (0.455), TTOP (0.654℃) and surface SM (0.309 cm^3/cm^3), whereas the PF zone exhibited the lowest mean NDVI (0.299), TTOP (−1.260℃) and surface SM (0.242 cm^3/cm^3); the PF to SFG zone had moderate mean NDVI (0.356), TTOP (−0.902℃) and surface SM (0.247 cm^3/cm^3) values. The average growing season NDVI from 1982 to 2015 decreased gradually from southeast to northwest in the SRYR, and the NDVI in the SFG was higher than that in the PF (Fig. 5). Relatively speaking, the hydrothermal conditions in the SFG zone for vegetation growth were far better than those in the PF zone.

From 1980 to 2015, the growing season NDVI in the SRYR generally increased with a mean change rate of 0.002 /10yr (Fig. 6a). An increasing NDVI trend occurred in 55.73% of the study area, with 30.99% showing significant increasing trends ($P < 0.05$). These areas were mainly found in the northern and other parts of the SRYR. The NDVI for the PF to SFG zone exhibited the greatest increasing trend, with a rate of 0.0034/10yr (the area with an increasing trend accounted for 60.59%). Moreover, the NDVI results in the PF and SFG zones showed increasing trends of 0.0026/10yr (58.11%) and 0.0031/10yr (54.79%), respectively. In the context of climate warming, the average ALT in the PF zone increased at a rate of 3.47 cm/yr (Fig. 6b). The regions with an extremely significant increase ($P < 0.05$) in ALT accounted for 36.02% and were mainly distributed in the western and southeastern SRYR. Rapid changes in ALT increases (3.60–4.00 cm/yr) were associated with the greatest increasing NDVI in this zone (0.006–0.008/10yr). The average SFD of seasonally frozen soil decreased at a rate of 0.93 cm/yr from 1980 to 2018 (Fig. 6c). Pixels with a significant decreasing rate in the SFD mainly occurred in the southeastern, northeastern and westernmost areas with SFG, 42.87% and 45.30% of the SFG zone and PF to SFG zone, respectively. In the area with the largest decreasing rate (< −1.40 cm/yr), the NDVI decreased or increased slightly.

The growing season TTOP and surface SM trends were heterogeneous across the three frozen ground zones. The TTOP increased in almost all pixels (99.90%) at a rate of 0.018℃/yr (Fig. 6d), with 0.022, 0.016 and 0.017℃/yr occurring in the SFG zone, PF to SFG zone and PF zone, respectively. The regions with the highest increasing rates occurred in the southeastern area of the SFG zone, while the lowest rates occurred in the central part of the SRYR. The increasing trends in the TTOP were 0.22, 0.19 and 0.15℃/yr in the SFG zone,

Table 4 Mean values and trends of the ALT, SFD, growing season NDVI, TTOP and SM in the three frozen ground zones of the source region of Yellow River during the study period

Zuoqi	ALT		SFD		NDVI		TTOP		SM	
	Mean (cm)	Trend (cm/yr)	Mean (cm)	Trend (cm/yr)	Mean	Trend (/10yr)	Mean (℃)	Trend (℃/yr)	Mean (cm^3/cm^3)	Trend ($cm^3/(cm^3 \cdot yr)$)
PF	228.948	3.472*	—	—	0.299	0.0026*	−1.260	0.017*	0.242	0.0002
PF to SFG	—	—	201.841	−0.601*	0.356	0.0034*	−0.902	0.016*	0.247	0.0016*
SFG	—	—	186.827	−0.567*	0.455	0.0031*	0.654	0.022*	0.309	−0.0013*

Note: ALT, SFD, NDVI, TTOP and SM are the active layer thickness or soil thawing depth of permafrost soil, the soil freezing depth of seasonal frozen soil, normalized difference vegetation index in growing season, the temperature at the bottom of the active layer and surface soil moisture, respectively. The zones of PF, PF to SFG and SFG represent the permafrost, the area where permafrost degrade into seasonally frozen ground and seasonally frozen ground, respectively. Time series of frozen ground factors (ALT, SFD, TTOP), NDVI and SM are for the period of 1980–2018, 1982–2015 and 2003–2011, respectively.* is significant at the level of 0.05

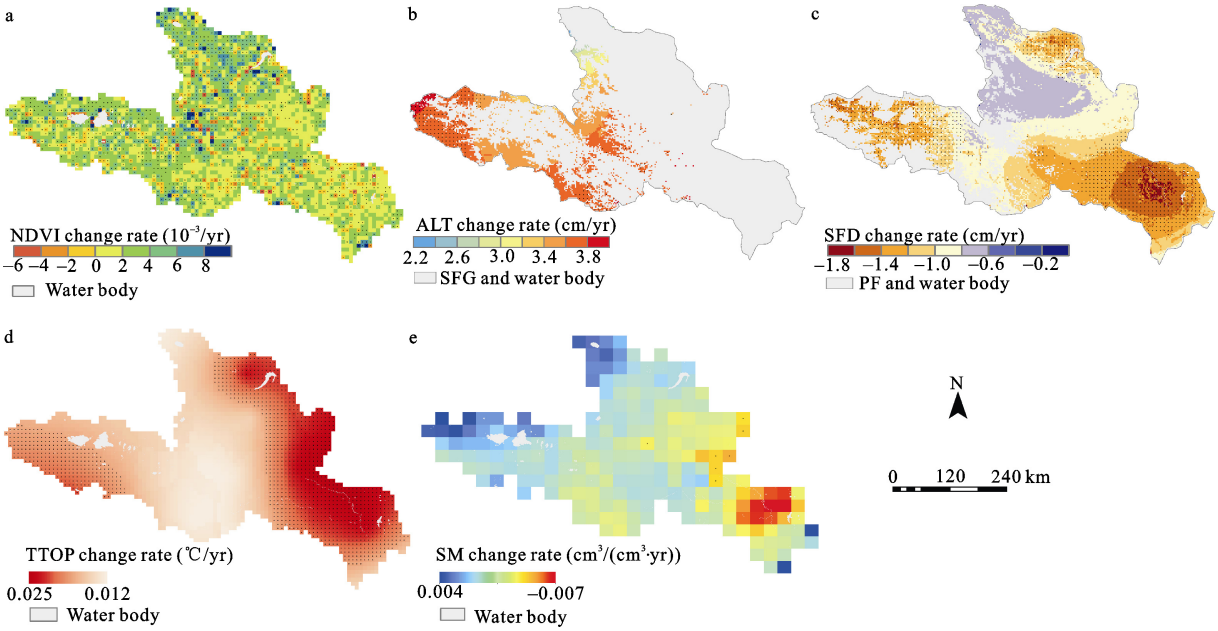

Fig. 6 Spatial distributions of the trends of normalized difference vegetation index (NDVI) in the growing season (a), the active layer thickness or soil thawing depth of permafrost soil (ALT) (b), the soil freezing depth of seasonal frozen soil (SFD) (c) and the temperature at the bottom of the active layer (TTOP) (d) and the surface soil moisture (SM) (e) in the source region of the Yellow River. Time series of frozen ground factors (ALT, SFD, TTOP), NDVI and SM are for the period of 1980–2018, 1982–2015 and 2003–2011, respectively.The black dots in the figures represent trends that were statistically significant at the 0.05 level

PF to SFG zone and PF zone, respectively. The SM showed a generally decreasing trend in the SRYR, with a rate of 0.0012 cm^3/(cm^3·yr) from 2003 to 2010 (Fig. 6e). The SFG zone, which had higher initial SM, showed a decreasing trend (0.0013 cm^3/(cm^3·yr)), whereas the PF zone and PF to SFG zone, which had lower initial values, showed increasing trends of 0.0002 and 0.0016 cm^3/(cm^3·yr), respectively.

3.3 Relationship between NDVI and frozen soil factors

Pearson correlation was used between the growing season NDVI and ALT of PF soil and SFD of seasonally frozen soil (Fig. 7). The growing season NDVI in the PF zones showed a positive correlation with the ALT in a majority of the pixels (65.97%) (Fig. 7a). The significant positive correlation (23.74%) was mainly located in the western and southeastern part of the PF zone, with the greatest increasing trend in ALT, whereas the significantly negative correlation (6.09%) was distributed randomly. The NDVI was negatively correlated with the SFD in 61.84% of the SFG and PF to SFG zones (Fig. 7b). Approximately 18.68% of the NDVI pixels showed a significant negative correlation with the SFD, which mainly occurred in the northern and middle areas of the SFG zone with a change rate in SFD (> −1.4 cm/yr). The significantly positive correlation (6.5%) was mainly located in the southeastern SFG zone, where the greatest change rate in SFD (< −1.4 cm/yr) occurred. Table 5 shows that the growing season NDVI exhibited significantly positive correlations with the TTOP and SM across all three frozen ground types, and the correlation coefficients were lower than those with ALT and SFD. However, the correlation coefficients between NDVI and SM were greater than those between NDVI and TTOP.

To further explore the potential hydrothermal effects of frozen ground degradation on vegetation growth, the correlations of ALT and SFD with TTOP and SM were also assessed at the pixel scale (Fig. 8). Clearly, an increase in ALT and decrease in SFD were associated with an increase in TTOP, producing a favorable thermal effect on vegetation recovery in this region (Fig. 8a and 8c). The variations in ALT and SFD exhibited a complex relationship with changes in SM (Fig. 8b and 8d). The greatest decrease in SFD (<−1.4 cm/yr) resulted in a decrease in SM. The modest change rate in SFD (>−1.4 cm/yr) was positively correlated with an increase in SM and therefore could have facilitated vegetation growth. However, the increase in ALT had a weak correlation with SM.

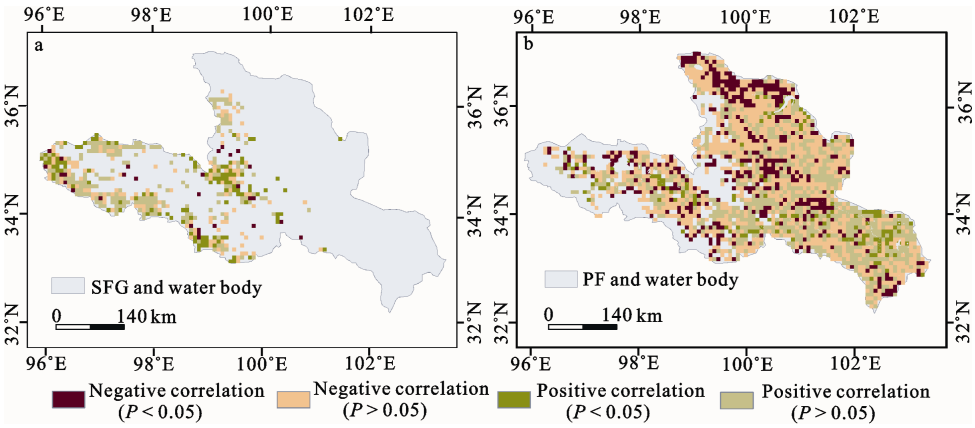

Fig. 7 Correlation between normalized difference vegetation index (NDVI) and soil thawing depth of permafrost soil (ALT) (a), NDVI and soil freezing depth of seasonal frozen soil (SFD) in the area where permafrost degrade into seasonally frozen ground (PF to SFG zone) and seasonally SFG (b) from 1982 to 2015 in the source region of the Yellow River

Table 5 Correlation coefficients between the growing season normalized difference vegetation index (NDVI) and frozen soil factors in the source region of the Yellow River

Zone	ALT	SFD	TTOP	SM
PF	0.518**	—	0.496**	0.552*
PF to SFG	—	−0.556**	0.507**	0.528**
SFG	—	−0.738**	0.396*	0.674**

Notes: ALT, SFD, TTOP and SM are the soil thawing depth of permafrost soil, the soil freezing depth of seasonal frozen soil, the temperature at the bottom of the active layer and surface soil moisture, respectively. The zones of PF, PF to SFG and SFG represent the permafrost, the area where permafrost degrade into seasonally frozen ground and seasonally frozen ground, respectively. * and ** are significant at the levels of 0.05 and 0.01, respectively

3.4 Comparisons of vegetation growth for different vegetation types

The trends in the growing season NDVI and frozen soil factors (including the ALT, SFD, TTOP and SM) for six types of vegetation and the correlation coefficients between the NDVI and frozen soil factors for different frozen ground types are listed in Table 6. Most of the vegetation types (except shrubs and barren land in the PF and PF to SFG zones and steppe in the SFG zone) showed an increasing trend in the growing season from 1982 to 2015. NDVI of meadow in the PF to SFG zone had the largest significant increasing trend, with a rate of 0.050/10a, followed by alpine vegetation in the SFG and PF to SFG zones, with increasing rates of 0.013/10a and 0.012/10a, respectively. The NDVI significantly increased for meadows in all frozen ground zones. Steppe had an increasing trend in both the PF zone and PF to SFG zone but showed a significant decreasing trend at a rate of 0.004/10a in the SFG zone. Significant increases in TTOP occurred for all vegetation types from 1982 to 2015, but SM mainly decreased from 2003 to 2011.

With the exception of shrubs and barren land, the NDVI for most vegetation types was positively correlated with the ALT in the PF zone. Almost all the vegetation types (except for steppe in the SFG zone and shrubs and barren land in the PF to SFG zone) exhibited positive correlations with SFD in the SFG and PF to SFG zones. For meadows in the SRYR, NDVI had a stronger correlation with SFD, ALT and TTOP than with SM across all three frozen ground types. The steppe NDVI showed a stronger relationship with SFD, ALT and SM than with TTOP. In addition, an increasing TTOP was positively associated with the growing season NDVI for most vegetation types, except for shrubs in the PF and PF to SFG zones, barren land in all three zones and steppe in the SFG zone. The trends in SM varied among the frozen ground types and vegetation groups, and thus, the relationships between NDVI and SM were quite different. Steppe presented a positive correlation with SM in the PF and PF to SFG zones but a negative correlation in the SFG zone, exhibiting the greatest significant correlation compared with the other vegetation types.

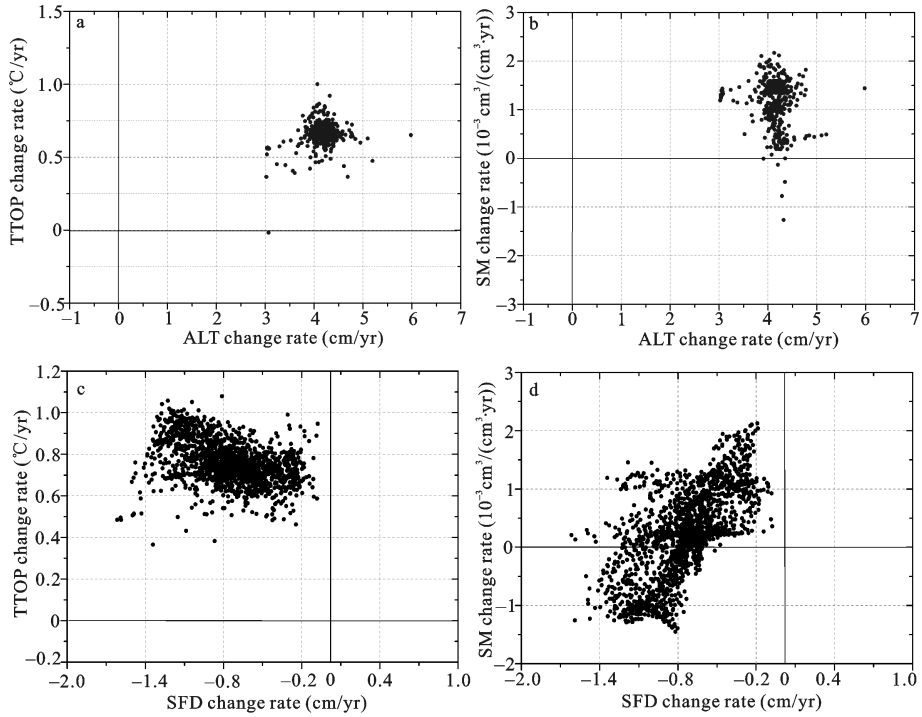

Fig. 8 Correlation analysis between the change rates in the active layer thickness of permafrost soil (ALT) and the temperature at the bottom of the active layer (TTOP) (a), ALT and surface soil moisture (SM) (b), the soil freezing depth of seasonal frozen soil (SFD) and TTOP (c) and SFD and SM (d)

Table 6 The trends of the growing season normalized difference vegetation index (NDVI) and frozen soil factors for six types of vegetation and the correlation coefficients between NDVI and frozen soil factors for different frozen ground types in the source region of the Yellow River

Zone	Vegetation	Linear trend					Correlation coefficient			
		NDVI (/10yr)	ALT (cm/yr)	SFD (cm/yr)	TTOP (℃/yr)	SM (cm^3/(cm^3·10yr))	R_{ALT}	R_{SFD}	R_{TTOP}	R_{SM}
PF	Shrub	−0.003	3.710**		0.142**	−0.020**	−0.055		−0.218*	0.145
	Steppe	0.006**	4.180**		0.151**	0.037**	0.441**		0.318**	0.402**
	Meadow	0.003	4.450**		0.174**	0.002	0.364**		0.367**	0.243
	Alpine vegetation	0.004**	4.090**		0.171**	−0.031**	0.376**		0.378**	−0.257**
	Barren land	−0.012**	4.030**		0.168**	0.003	−0.238		−0.365**	−0.193
SFG	Forest	0.004**		−0.500**	0.146**	−0.018**		−0.312**	0.252	−0.241
	Shrub	0.008**		−0.500**	0.178**	−0.023**		−0.362**	0.202	−0.382**
	Steppe	−0.004**		−0.580**	0.186**	−0.013*		0.493**	−0.434**	0.644**
	Meadow	0.006**		−0.550**	0.184**	−0.023**		−0.454**	0.436**	−0.322*
	Alpine vegetation	0.013**		−0.560**	0.193**	−0.015*		−0.488**	0.675**	−0.462**
	Barren land	0.009**		−0.550**	0.203**	−0.008*		−0.593**	−0.478**	−0.519**
PF to SFG	Shrub	−0.005**		−0.530**	0.174**	0.011*		0.226*	−0.338**	−0.409**
	Steppe	0.010**		−0.530**	0.180**	0.017**		−0.475**	0.378**	0.559**
	Meadow	0.050**		−0.570**	0.204**	−0.026*		-0.542**	0.508**	−0.409**
	Alpine vegetation	0.012**		−0.550**	0.187**	0.015*		−0.511**	0.488**	0.196
	Barren land	−0.005**		−0.540**	0.179**	−0.012*		0.131	−0.282	0.398**

Notes: ALT, SFD, NDVI, TTOP and SM are the active layer thickness or soil thawing depth of permafrost soil, the soil freezing depth of seasonal frozen soil, normalized difference vegetation index, the temperature at the bottom of the active layer and surface soil moisture, respectively. The zones of PF, SFG and PF to SFG represent the permafrost, seasonally frozen ground and the area where permafrost degrade into seasonally frozen ground, respectively. Time series of NDVI, frozen ground factors (ALT, SFD, TTOP) and SM are for the period of 1982−2015, 1980−2018 and 2003−2011, respectively. * and ** represent significant at the levels of 0.05 and 0.01 for linear trend and correlation coefficient, respectively

4 Discussion

4.1 Frozen ground degradation and vegetation growth

In a warming climate in the SRYR, the distribution of PF has been shrinking, and the distribution of SFG has been expanding over the past few decades. By using the TTOP model, the study area was divided into three zones, namely, PF, SFG and PF to SFG, to investigate the effects of frozen ground changes on vegetation growth. The spatiotemporal characteristics of the NDVI across different frozen ground types were compared, which provided a new understanding of the vegetation dynamics in the SRYR in recent years. In this study, vegetation NDVI exhibited increasing trends in all three frozen ground types from 1982 to 2015, which is consistent with previous studies at the regional scale based on remote sensing data (Yang et al., 2013; Pang et al., 2017). This increasing trend indicated that variations in frozen ground conditions might have improved vegetation. However, several observations from field surveys at the plot scale resulted in opposite conclusions: frozen ground degradation under climate warming resulted in the degradation of alpine grassland, including a decrease in its distribution, vegetation coverage and species richness and a reversed community succession (Wang et al., 2016). These results may have differed due to different observation methods, study areas and time intervals (Xu et al., 2011).

Fig. 6a demonstrates that the vegetation greening trend increased from the PF zone to the SFG zone and was greatest in the transition zone (PF to SFG zone), which was similar to the results from Yi et al. (2011) and Qin et al. (2017). In PF regions in Northeast China, the increasing trend in vegetation varied among continuous PF, discontinuous PF with island taliks and sparse islands in the PF zone (Guo et al., 2017). Differences in geological features and physical freezing and thawing processes existed between seasonally frozen soil and PF soil, resulting in discrepancies in hydrothermal characteristics (Gu et al., 2015). The present study showed that the TTOP and SM conditions in the SFG zone with a lower altitude, were better than those in the PF zone, and therefore, the mean annual NDVI value in the SFG zone was much higher. Vegetation greening trends will be enhanced by the warming of frozen soil and the increase in soil water content during the thawing and freezing seasons, potentially extending the growing season period (Stow et al., 2003). Therefore, the differences in vegetation trends could be explained by variations in hydrothermal conditions within frozen ground degradation.

4.2 Frozen ground factors influencing the vegetation growth

As integrated hydrothermal factors, the depths of seasonal freezing and thawing (ALT and SFD) strongly affect vegetation growth and activity. In this study, we paid special attention to the relationships of the NDVI, ALT, SFD, TTOP and SM. The correlation coefficients showed that an increase in ALT and a decrease in SFD had a positive effect on increasing the NDVI in the SRYR (Table 5), which was similar to previous studies (Cuo et al., 2015; Qin et al., 2017). The results of other studies, however, contrasted with these outcomes (Jin et al., 2009; Wang et al., 2012; Iijima et al., 2014). Clearly, a decrease in SFD and an increase in ALT as a result of increasing temperature appear to mitigate the low-temperature stress of vegetation growth in cold regions. Our study agreed with these results: the correlation coefficients between the growing season NDVI and TTOP were significantly positive (Table 5). However, SM availability might decline because of greater evapotranspiration with increasing temperature, resulting in complicated relationships between vegetation and temperature (Mowll et al., 2015). Many previous studies showed that the effect of water on vegetation was considerably greater than that of heat in this region (Hu et al., 2011), which is consistent with our results. In our study, the correlation between SM and NDVI in the SFG zone was stronger than that between TTOP and NDVI.

In comparison, the SM for the SFG and PF to SFG zones increased with a modest decrease in SFD (<−1.4 cm/yr) and decreased with the greatest decrease in SFD (> −1.4 cm/yr) (Fig. 8d). The spatial discrepancies were associated with different soil types and the lowering of the water table during seasonal freezing-thawing process (Qin et al., 2017). Generally, the thermal conductivity of fine soil, which has high water-holding capability, is less than that of coarse soil, and thus, the latter has a lower SFD (Wang et al., 2017a). A seasonal freezing process with a lower freezing rate appears to be much more conducive to moisture migration and ice segregation (Rode et al., 2016). In addition, the largest decrease in SFD was mainly attributed to rising temperatures, resulting in an increase in evapotranspiration and loss of

SM. Because the increase change rate of SFD in the SFG zone was greater than that in the PF to SFG zone (Table 4 and Fig. 7), the moisture condition in the PF to SFG zone was much favorable for vegetation growth.

4.3 Responses of vegetation growth to frozen ground degradation under different vegetation types

In addition to the frozen ground types, the responses of vegetation to frozen ground degradation in the SRYR differed among vegetation types. Meadow and steppe are the primary ecosystems in the SRYR. For meadows in the SRYR, the NDVI had a stronger correlation with SFD, ALT and temperature than moisture across all three frozen ground types (Table 6). Although the SM of meadows in the SFG and PF to SFG zones showed a decreasing trend while increasing in the PF zone, the NDVI still demonstrated an increasing trend. This pattern indicated that the meadow system in this region was limited by thermal effect induced by increasing temperature, the shrinking distribution of PF area and variations in ALT and SFD. This finding was consistent with previous results for alpine meadows on the plateau (Ganjurjav et al., 2016). As humid systems, meadows have sufficient soil water availability due to low respiration and a fine soil texture (Guo et al., 2015; Zhang et al., 2017). Therefore, the more important factors affecting meadows were likely thermal factors, while moisture appeared to be less important.

Scott et al. (2010) suggested that steppes have lower levels of SM and drier climates than alpine meadow areas and are thus more sensitive to SM, which is similar to our results. Our study showed that SM, ALT and SFD had a large influence on steppe NDVI for all three frozen ground types compared to the temperature. This result implied that increasing moisture induced by variations in the active layers favored the improvement of steppe vegetation. Moreover, the steppe NDVI demonstrated an increasing trend in the PF and PF to SFG zones but a decreasing trend in the SFG zone. This finding may be explained by decreasing SM along with the greatest thinning SFD, which eventually reduced the NDVI in the SFG zone.

4.4 Limitations of this study

In this study, the TTOP model and Stefan equation were used to detect the distribution of frozen ground and simulate the depths of seasonal freezing and thawing. However, the available meteorological stations were sparse and unevenly distributed because of the variable terrain and transboundary nature of the study area, so uncertainties may have occurred during the estimation processes. Although SM plays an important role in the response of vegetation to frozen ground degradation, the availability of SM data derived from AMSR-E from 2003 to 2011 was limited. If the period with SM data was consistent with the NDVI dataset, the results would be more convincing because more data would decrease the effect of random factors. In addition, the classification of vegetation types that was used in this study was conducted in 2000, but the land use and vegetation types might have changed greatly in recent years. Furthermore, vegetation growth is also affected by human activities in the SRYR, especially overgrazing, which were not considered in the present study and require further investigation.

5 Conclusions

Based on regional-scale decadal variations in types of frozen ground, the depths of seasonal freezing/thawing, vegetation NDVI, TTOP, and surface SM, we discriminated the different responses of vegetation to frozen ground degradation for different types of frozen ground and vegetation. Over the past four decades, approximately 20.37% of the SRYR in the 1980s was projected to degrade into SFG in the 2010s. As indicators of PF, PF to SFG and SFG zones, the average ALT increased at a rate of 3.47 cm/yr from 1980 to 2018 and the average SFD decreased at a rate of 0.93 cm/yr. The growing season NDVI increased in 55.73% of the study area at a rate of 0.002/10yr from 1982 to 2015.

For different frozen ground types, the proportion of areas with vegetation greening and improving rate increased from the PF zone to the SFG zone and was greatest in the transition zone (PF to SFG zone). A correlation analysis showed that the growing season NDVI had a significant positive correlation with ALT in the PF zone but a negative correlation with SFD in the SFG and PF to SFG zones. SM played a crucial role in the response of vegetation growth to variations in ALT and SFD. The rapid decrease in SFD (< -1.4 cm/yr) might have reduced the surface SM and thus decreased the NDVI.

For different vegetation types, most of them (except for shrubs and barren land in the PF and PF to SFG zones and steppe in the SFG zone) showed increasing trends in the growing season from 1982 to 2015. The NDVI of those vegetation types exhibited a significant positive correlation with ALT and a negative correlation with SFD. Meadow NDVI was mainly limited by thermal factors induced by increasing TTOP and variations in ALT and SFD. In contrast, steppe was mainly limited by hydrological factors that involved variations in SM alongside frozen ground degradation.

Acknowledgement

We would like to thank the National Meteorological Information Center, the Geospatial Data Cloud, and the Cold and Arid Regions Science Data Center in Lanzhou for providing meteorological data, DEM, vegetation types and frozen ground type data.

References

Anderson J E, Douglas T A, Barbato R A et al., 2019. Linking vegetation cover and seasonal thaw depths in interior Alaska permafrost terrains using remote sensing. *Remote Sensing of Environment*, 233: 111363. doi: 10.1016/j.rse.2019.111363

Barry R G, Gan T Y, 2011. *The Global Cryosphere: Past*, *Present and Future*. Cambridge: Cambridge University Press.

Cable J M, Ogle K, Bolton W R et al., 2014. Permafrost thaw affects boreal deciduous plant transpiration through increased soil water, deeper thaw, and warmer soils. *Ecohydrology*, 7(3): 982–997. doi: 10.1002/eco.1423

Cuo L, Zhang Y X, Bohn T J et al., 2015. Frozen soil degradation and its effects on surface hydrology in the northern Tibetan Plateau. *Journal of Geophysical Research: Atmospheres*, 120(16): 8276–8298. doi: 10.1002/2015JD023193

Dente L, Vekerdy Z, Wen J et al., 2012. Maqu network for validation of satellite-derived soil moisture products. *International Journal of Applied Earth Observation and Geoinformation*, 17: 55–65. doi: 10.1016/j.jag.2011.11.004

Du Jiaqiang, Shu Jianmin, Wang Yurhui et al., 2014. Comparison of GIMMS and MODIS normalized vegetation index composite data for Qinghai-Tibet Plateau. *Chinese Journal of Applied Ecology*, 25(2): 533–544. (in Chinese)

Evans S G, Ge S M, 2017. Contrasting hydrogeologic responses to warming in permafrost and seasonally frozen ground hillslopes. *Geophysical Research Letters*, 44(4): 1803–1813. doi: 10.1002/2016GL072009

Food and Agriculture Organization of the United Nations (FAO), World Soil Information, Institute of Soil Science (ISRIC), Joint Research Centre of the European Commission (JRC), 2009. Harmonized World Soil Database (Version 1.1). Available at: http://www.fao.org/land-water/databases-and-software/hwsd/en/

Feng Y Q, Liang S H, Kuang X X et al., 2019. Effect of climate and thaw depth on alpine vegetation variations at different permafrost degrading stages in the Tibetan Plateau, China. *Arctic*, *Antarctic*, *and Alpine Research*, 51(1): 155–172. doi: 10.1080/15230430.2019.1605798

Frauenfeld O W, Zhang T J, 2011. An observational 71-year history of seasonally frozen ground changes in the Eurasian high latitudes. *Environmental Research Letters*, 6(4): 044024. doi: 10.1088/1748-9326/6/4/044024

Ganjurjav H, Gao Q Z, Gornish E S et al., 2016. Differential response of alpine steppe and alpine meadow to climate warming in the central Qinghai-Tibetan Plateau. *Agricultural and forest Meteorology*, 223: 233–240. doi: 10.1016/j.agrformet.2016.03.017

Gao B, Yang D W, Qin Y et al., 2018. Change in frozen soils and its effect on regional hydrology, upper Heihe basin, northeastern Qinghai-Tibetan Plateau. *The Cryosphere*, 12(2): 657–673. doi: 10.5194/tc-12-657-2018

Gu L L, Yao J M, Hu Z Y et al., 2015. Comparison of the surface energy budget between regions of seasonally frozen ground and permafrost on the Tibetan Plateau. *Atmospheric Research*, 153: 553–564. doi: 10.1016/j.atmosres.2014.10.012

Guo D L, Wang H J, 2013. Simulation of permafrost and seasonally frozen ground conditions on the Tibetan Plateau, 1981–2010. *Journal of Geophysical Research*: *Atmospheres*, 118(11): 5216–5230. doi: 10.1002/jgrd.50457

Guo J T, Hu Y M, Xiong Z P et al., 2017. Variations in growing-season NDVI and its response to permafrost degradation in Northeast China. *Sustainability*, 9(4): 551. doi: 10.3390/su9040551

Guo Q, Hu Z M, Li S G et al., 2015. Contrasting responses of gross primary productivity to precipitation events in a water-limited and a temperature-limited grassland ecosystem. *Agricultural and Forest Meteorology*, 214–215: 169–177. doi: 10.1016/j.agrformet.2015.08.251

Hou Xueyu, 2001. *Vegetation Atlas of China (1: 1000000)*. Beijing: Science Press. (in Chinese)

Hu M Q, Mao F, Sun H et al., 2011. Study of normalized difference vegetation index variation and its correlation with climate factors in the Three-River-Source region. *International Journal of Applied Earth Observation and Geoinformation*, 13(1): 24–33. doi: 10.1016/j.jag.2010.06.003

Iijima Y, Ohta T, Kotani A et al., 2014. Sap flow changes in relation to permafrost degradation under increasing precipitation in an eastern Siberian larch forest. *Ecohydrology*, 7(2): 117–187. doi: 10.1002/eco.1366

Jin H J, He R X, Cheng G D et al., 2009. Changes in frozen ground in the Source Area of the Yellow River on the Qinghai–Tibet Plateau, China, and their eco-environmental impacts. *Environmental Research Letters*, 4(4): 045206. doi: 10.1088/1748-9326/4/4/045206

Klanderud K, 2008. Species-specific responses of an alpine plant community under simulated environmental change. *Journal of*

Vegetation Science, 19(3): 363–372. doi: 10.3170/2008-8-18376

Lawrence D M, Slater A G, Swenson S C, 2012. Simulation of present-day and future permafrost and seasonally frozen ground conditions in CCSM4. *Journal of Climate*, 25(7): 2207–2225. doi: 10.1175/JCLI-D-11-00334.1

Luo D L, Jin H J, Marchenko S et al., 2014. Distribution and changes of active layer thickness (ALT) and soil temperature (TTOP) in the source area of the Yellow River using the GIPL model. *Science China Earth Sciences*, 57(8): 1834–1845. doi: 10.1007/s11430-014-4852-1

Miranda V, Pina P, Heleno S et al., 2020. Monitoring recent changes of vegetation in Fildes Peninsula (King George Island, Antarctica) through satellite imagery guided by UAV surveys. *Science of the Total Environment*, 704: 135295. doi: 10.1016/j.scitotenv.2019.135295

Mowll W, Blumenthal D M, Cherwin K et al., 2015. Climatic controls of aboveground net primary production in semi-arid grasslands along a latitudinal gradient portend low sensitivity to warming. *Oecologia*, 177(4): 959–969. doi: 10.1007/s00442-015-3232-7

Mu C C, Li L L, Zhang F et al., 2018. Impacts of permafrost on above-and belowground biomass on the northern Qinghai-Tibetan Plateau. *Arctic*, *Antarctic*, *and Alpine Research*, 50(1): e1447192. doi: 10.1080/15230430.2018.1447192

Oliva M, Pereira P, Antoniades D, 2018. The environmental consequences of permafrost degradation in a changing climate. *Science of the Total Environment*, 616–617: 435–437. doi: 10.1016/j.scitotenv.2017.10.285

Pan F F, Peters-Lidard C D, Sale M J, 2003. An analytical method for predicting surface soil moisture from rainfall observations. *Water Resources Research*, 2003, 39(11): 1314. doi: 10.1029/2003wr002142

Qin Dahe, Stocker T, 2014. Highlights of the IPCC working group I fifth assessment report. *Progressus Inquisitiones de Mutatione Climatis*, 10(1): 1–6. (in Chinese)

Qin Y, Yang D W, Gao B et al., 2017. Impacts of climate warming on the frozen ground and eco-hydrology in the Yellow River source region, China. *Science of the Total Environment*, 605–606: 830–841. doi: 10.1016/j.scitotenv.2017.06.188

Ran Y H, Li X, Lu L et al., 2012. Large-scale land cover mapping with the integration of multi-source information based on the dempster-shafer theory. *International Journal of Geographical Information Science*, 26(1): 169−191. doi: 10.1080/13658816.2011.577745

Rode M, Schnepfleitner H, Sass O, 2016. Simulation of moisture content in alpine rockwalls during freeze-thaw events. *Earth Surface Processes and Landforms*, 41(13): 1937–1950. doi: 10.1002/esp.3961

Scott R L, Hamerlynck E P, Jenerette G D et al., 2010. Carbon dioxide exchange in a semidesert grassland through drought–induced vegetation change. *Journal of Geophysical Research: Biogeosciences*, 115(G3): G03026. doi: 10.1029/2010JG001348

Shen X J, An R, Feng L et al., 2018. Vegetation changes in the Three-River Headwaters Region of the Tibetan Plateau of China. *Ecological Indicators*, 93: 804–812. doi: 10.1016/j.ecolind.2018.05.065

Smith M W, Riseborough D W, 1996. Permafrost monitoring and detection of climate change. *Permafrost and Periglacial Processes*, 7(4): 301–309. doi: 10.1002/(SICI)1099-1530(199610)7:4<301: AID-PPP231>3.0.CO;2-R

Stow D, Daeschner S, Hope A et al., 2003. Variability of the seasonally integrated normalized difference vegetation index across the north slope of Alaska in the 1990s. *International Journal of Remote Sensing*, 24(5): 1111–1117. doi: 10.1080/0143116021000020144

Walker M D, Wahren C H, Hollister R D et al, 2006. Plant community responses to experimental warming across the tundra biome. *Proceedings of the National Academy of Sciences of the United States of America*, 103(5): 1342–1346. doi: 10.1073/pnas.0503198103

Wang Q F, Zhang T J, Jin H J et al., 2017a. Observational study on the active layer freeze-thaw cycle in the upper reaches of the Heihe River of the north-eastern Qinghai-Tibet Plateau. *Quaternary international zhengti*, 440: 13–22. doi: 10.1016/j.quaint. 2016.08.027

Wang R, Dong Z B, Zhou Z C, 2019a. Changes in the depths of seasonal freezing and thawing and their effects on vegetation in the Three-River Headwater Region of the Tibetan Plateau. *Journal of Mountain Science*, 16(12): 2810–2827. doi:10.1007/s11629-019-5450-7.

Wang R, Dong Z B, Zhou Z C, 2020. Effect of decreasing soil frozen depth on vegetation growth in the source region of the Yellow River. *Theoretical and Applied Climatology*. doi: 10.1007/s00704-020-03141-3 (in press)

Wang R, Zhu Q K, Ma H et al., 2017b. Spatial-temporal variations in near-surface soil freeze-thaw cycles in the source region of the Yellow River during the period 2002–2011 based on the Advanced Microwave Scanning Radiometer for the Earth Observing System (AMSR-E) data. *Journal of Arid Land*, 9(6): 850–864. doi: 10.1007/s40333-017-0032-4

Wang R, Zhu Q K, Ma H, 2019b. Changes in freezing and thawing indices over the source region of the Yellow River from 1980 to 2014. *Journal of Forestry Research*, 30(1): 257–268. doi: 10.1007/s11676-017-0589-y

Wang T H, Yang D W, Qin Y et al., 2018a. Historical and future changes of frozen ground in the upper Yellow River Basin. *Global and Planetary Change*, 162: 199–211. doi: 10.1016/j.gloplacha.2018.01.009

Wang T Y, Wu T H, Wang P et al., 2019c. Spatial distribution and changes of permafrost on the Qinghai-Tibet Plateau revealed by statistical models during the period of 1980 to 2010. *Science of the Total Environment*, 650: 661–670. doi: 10.1016/j.scitotenv.2018.08.398

Wang X Y, Yi S H, Wu Q B et al., 2016. The role of permafrost and soil water in distribution of alpine grassland and its NDVI dynamics on the Qinghai-Tibetan Plateau. *Global and Planetary Change*, 147: 40–53. doi: 10.1016/j.gloplacha.2016.10.014

Wang Y H, Yang H B, Gao B et al., 2018b. Frozen ground degradation may reduce future runoff in the headwaters of an inland river on the northeastern Tibetan Plateau. *Journal of Hydrology*, 564: 1153–1164. doi: 10.1016/j.jhydrol.2018.07.078

Wang Z R, Yang G J, Yi S H et al., 2012. Different response of vegetation to permafrost change in semi-arid and semi-humid regions in Qinghai-Tibetan Plateau. *Environmental Earth Sciences*, 66(3): 985–991. doi: 10.1007/s12665-011-1405-1

Woo M K, 2012. *Permafrost Hydrology*. Heidelberg: Springer.

Wu Q B, Hou Y D, Yun H B et al., 2015. Changes in active-layer thickness and near-surface permafrost between 2002 and 2012 in alpine ecosystems, Qinghai-Xizang (Tibet) Plateau, China. *Global and Planetary Change*, 124: 149–155. doi: 10.1016/j.gloplacha.2014.09.002

Xu W X, Gu S, Zhao X Q et al., 2011. High positive correlation between soil temperature and NDVI from 1982 to 2006 in alpine meadow of the Three-River Source Region on the Qinghai-Tibetan Plateau. *International Journal of Applied Earth Observation and Geoinformation*, 13(4): 528–535. doi: 10.1016/j.jag.2011.02.001

Yang M X, Wang X J, Pang G J et al., 2019. The Tibetan Plateau cryosphere: Observations and model simulations for current status and recent changes. *Earth Science Reviews*, 190: 353–369. doi: 10.1016/j.earscirev.2018.12.018

Yang M X, Wang X J, Pang G J et al., 2019. The Tibetan Plateau cryosphere: observations and model simulations for current status and recent changes. *Earth-Science Reviews*, 190: 353–369. doi: 10.1016/j.earscirev.2018.12.018

Yang Z H, Still B, Ge X X, 2015. Mechanical properties of seasonally frozen and permafrost soils at high strain rate. *Cold Regions Science and Technology*, 113: 12–19. doi: 10.1016/j.coldregions.2015.02.008

Yang Z P, Gao J X, Zhao L et al., 2013. Linking thaw depth with soil moisture and plant community composition: effects of permafrost degradation on alpine ecosystems on the Qinghai-Tibet Plateau. *Plant and Soil*, 367(1–2): 687–700. doi: 10.1007/s11104-012-1511-1

Yao Tandong, Qin Dahe, Shen Yongping et al., 2013. Cryospheric changes and their impacts on regional water cycle and ecological conditions in the Qinghai-Tibetan Plateau. *Chinese Journal of Nature*, 35(3): 179–186. (in Chinese)

Yi S H, Zhou Z Y, Ren S L et al., 2011. Effects of permafrost degradation on alpine grassland in a semi-arid basin on the Qinghai-Tibetan Plateau. *Environmental Research Letters*, 6(4): 45403. doi: 10.1088/1748-9326/6/4/045403

Zhang T, Wang G X, Yang Y et al., 2017. Grassland types and season-dependent response of ecosystem respiration to experimental warming in a permafrost region in the Tibetan Plateau. *Agricultural and Forest Meteorology*, 247: 271–279. doi: 10.1016/j.agrformet.2017.08.010

Zorigt M, Kwadijk J, Van Beek E et al., 2016. Estimating thawing depths and mean annual ground temperatures in the Khuvsgul region of Mongolia. *Environmental Earth Sciences*, 75(10): 897. doi: 10.1007/s12665-016-5687-1